Transaction A: Civil Engineering
Vol. 16, No. 6, pp. 512–519

Research Note

Nonlinear FE Analysis of Reinforced Concrete Structures Using a Tresca-Type Yield Surface

M. Nazem[1,*], I. Rahmani[2] and M. Rezaee-Pajand[3]

Abstract. *This paper presents a nonlinear analysis of reinforced concrete structures. Various yield surfaces of concrete are reviewed in the beginning and then a recently proposed yield surface for concrete is introduced. The yield surface considers the behavior of concrete in a three-dimensional stress state. Based on the yield surface, a nonlinear finite element formulation is provided to facilitate a three-dimensional analysis of reinforced concrete structures. An eight-node brick element is used in the analysis. Several numerical examples are given to show the ability of the yield surface in solving nonlinear reinforced concrete problems.*

Keywords: *Finite element method; Yield surface; Nonlinear analysis; Reinforced concrete.*

INTRODUCTION

Concrete is a material widely used nowadays in structures such as tall buildings, nuclear power plants and dams. An analysis of such structures is not possible by classical methods and moreover experimental studies are costly. Recent advances in numerical techniques have developed the finite element method by which the concrete structures can be studied. As a matter of fact, there are some limitations within implementing finite element methods for reinforced concrete structures. The main reason for these limitations is the complex behavior of concrete and subsequently its modeling. The complexity is caused by:

1. Nonlinear stress-strain relation of concrete under multi-axial stress conditions;
2. Strain softening and anisotropic stiffness reduction;
3. Progressive cracking caused by tensile stresses and strains;
4. Bond between concrete and reinforcements;
5. Aggregation interlocks and dowel action of reinforcements;
6. Time-dependant behaviors as creep and shrinkage.

Presenting a convenient model that can predict the behavior of concrete in all situations has been an active research subject for a long time and still is. The starting point to a materially nonlinear analysis of a structure is introducing a yield function that can predict the behavior of material under an imposed stress state. Several yield criteria have been suggested for concrete. A brief review of concrete yield surfaces will be presented in the following and a recently proposed yield surface will be represented. The yield surface is used in a finite element formulation to solve some nonlinear problems of reinforced concrete structures.

GENERAL YIELD CRITERIA OF CONCRETE

The strength of concrete under three-axial stress is a function of stress tensor. This strength is dependant on compressive, tensile and shear stress in concrete. The fracture criteria of concrete under a three-dimensional stress state will be studied in this paper. A general definition for fracture must be presented for this purpose. A concrete element is fractured when it reaches the ultimate load bearing capacity and can tolerate no more loads. There are two kinds of fracture for concrete, named ductile and brittle. A brittle fracture is initialized by tensile cracks, and concrete loses its

1. *Centre for Geotechnical and Material Modeling, The University of Newcastle, Newcastle, P.O. Box 2308, Australia.*
2. *Transportation Research Institute, Ministry of Road and Transportation, Tehran, P.O. Box 15875-7573, Iran.*
3. *Department of Civil Engineering, Ferdowsi University of Mashhad, Mashad, P.O. Box 9177948944, Iran.*
*. *Corresponding author. E-mail: majidreza.nazem@newcastle.edu.au*

Received 22 July 2008; received in revised form 20 April 2009; accepted 12 September 2009

strength in the normal direction to cracking. This fracture occurs when concrete is under high tensile stress. Ductile fracture, on the other hand, starts with compressive micro-cracking, and concrete loses most of its strength. Stress carried by concrete reduces as the strains increase. Several criteria have been suggested for concrete. These criteria are divided into five different groups based on their assumptions. These are: one-parameter, two-parameter, three-parameter, four-parameter and five-parameter groups.

The one-parameter models require only one material parameter to define the yield surface of concrete which can be either the compressive or tensile strength of the concrete. Rankine and Tresca are such models. According to Rankine's criterion, the fracture in concrete starts when one of the principal stresses (σ_1, σ_2 or σ_3) reaches the tensile strength (f'_t). This criterion neglects the effect of shear stresses in concrete. In Tresca's yield criterion, fracture occurs when the maximum shear stress reaches a critical value as K, being the yield stress of concrete in pure shear. This parameter can be obtained by a uniaxial test for ductile materials.

The strength of concrete in tension and compression is not the same. Therefore, the yield surface of concrete does not possess three axes of symmetry. In other words, one-parameter models cannot predict the behavior of concrete in a general state of stress and models with more parameters are required. Two well-known two-parameter models are the Mohr-Columb criterion and the Drucker-Prager criterion. According to the Mohr-Columb criterion, the shear strength of a material is a function of cohesion and normal stresses. For concrete, the Mohr-Columb criterion may be expressed in terms of compressive strength (f'_c) and tensile strength (f'_t) by the following equation:

$$\frac{f'_c}{f'_t}\sigma_1 - \sigma_3 = f'_c, \tag{1}$$

where σ_1 and σ_2 are, respectively, the major and minor principal stresses. The Mohr-Columb criterion has provided good results in the analysis of beams and slabs where the shear is critical. The corners of a Mohr-Columb criterion usually cause complexity in the numerical integration of stress-strain relations and returning the stress state onto the yield surface. Drucker and Prager overcame this drawback by presenting the following criterion:

$$f(I_1, J_2) = \alpha I_1 + \sqrt{J_2} - K = 0, \tag{2}$$

where I_1 is the first invariant of the stress tensor, J_2 represents the second invariant of the deviatoric stress tensor and α and K are material parameters (see [1] for more details).

The relation between octahedral shear stress (τ_{oct}) and octahedral normal stress (σ_{oct}) is linear in the Drucker-Prager model and the failure surface represents a circle on the π plane. The experimental results, however, show that this relation is not linear and the failure surface is not a circle. Therefore, three-parameter models have been introduced. William and Warnke [1] introduced a three-parameter criterion for the tensile region of concrete with low compressive stresses. The failure surface on the π plane is an ellipse in this criterion and the corners of the yield surface are curvilinear and continuous. Moreover, the yield surface possesses three axes of symmetry.

The William-Warnke three-parameter criterion was then modified into a five-parameter one by adding two degrees of freedom. Doing so, the criterion will be more effective for the compressive state of stresses. This criterion is defined by the following equations:

$$\frac{2J_2}{5\sqrt{f'_c}} = a_0 + a_1\frac{\sigma_{\text{oct}}}{f'_c} + a_2\left(\frac{\sigma_{\text{oct}}}{f'_c}\right)^2, \quad \text{(tension)}, \tag{3}$$

$$\frac{2J_2}{5\sqrt{f'_c}} = b_0 + b_1\frac{\sigma_{\text{oct}}}{f'_c} + b_2\left(\frac{\sigma_{\text{oct}}}{f'_c}\right)^2, \quad \text{(compression)}. \tag{4}$$

The unknown parameters, a_0, a_1, a_2, b_0, b_1 and b_2 are obtained from experimental tests. The above equations intersect on the hydrostatic axis at a known point, therefore, there are only five-parameters to be determined.

QUASI-TRESCA YIELD SURFACES

A class of yield surfaces can be found in the literature, based on the Tresca yield function [2]. The Tresca yield surface for plane problems can be expressed by the following equations:

$$F_1 = \sigma_1 - \sigma(k) = 0,$$

$$F_2 = -\sigma_2 - \sigma(k) = 0,$$

$$F_3 = \sigma_1 - \sigma_2 - \sigma(k) = 0,$$

$$F_4 = \sigma_2 - \sigma(k) = 0,$$

$$F_5 = -\sigma_1 - \sigma(k) = 0,$$

$$F_6 = -\sigma_1 + \sigma_2 - \sigma(k) = 0. \tag{5}$$

The projection of this yield surface on the π plane represents a hexagon with two axes of symmetry. The Tresca yield function assumes that the behavior of the material under tension and compression will be the same. To overcome this drawback, the first quasi-Tresca yield surface was proposed by Rezaee-Pajand [3]. Assuming a to be the ratio between the compressive strength and tensile strength of the material, the following equations can be written for the first quasi-Tresca yield surface:

$$F_1 = \sigma_1 - \sigma_0 = 0,$$

$$F_2 = -\sigma_2 - a\sigma_0 = 0,$$

$$F_3 = a\sigma_1 - \sigma_2 - a\sigma_0 = 0,$$

$$F_4 = \sigma_2 - \sigma_0 = 0,$$

$$F_5 = -\sigma_1 - a\sigma_0 = 0,$$

$$F_6 = -\sigma_1 + a\sigma_2 - a\sigma_0 = 0, \tag{6}$$

where σ_0 is the yield stress of the material and can be obtained from the uniaxial tensile test. The first quasi-Tresca yield surface is applicable to materials with different compressive and tensile characteristics (Figure 1).

A more generalized form of the first quasi-Tresca yield surface was presented by Weisgerber [4]. Two extra parameters, β_1 and β_2, representing the behavior of material under tension and compression, are used to define the second quasi-Tresca yield surface, as follows:

$$F_1 = \beta_1\sigma_1 + (1 - \beta_1)\sigma_2 - \beta_1\sigma(k) = 0,$$

$$F_2 = (\beta_2 - 1)\sigma_1 - \beta_2\sigma_2 - a\beta_2\sigma(k) = 0,$$

$$F_3 = a\sigma_1 - \sigma_2 - a\sigma(k) = 0,$$

$$F_4 = (1 - \beta_1)\sigma_1 + \beta_1\sigma_2 - \beta_1\sigma(k) = 0,$$

$$F_5 = -\beta_2\sigma_1 + (\beta_2 - 1)\sigma_2 - a\beta_2\sigma(k) = 0,$$

$$F_6 = -\sigma_1 + a\sigma_2 - a\sigma(k) = 0. \tag{7}$$

Parameters β_1 and β_2 are obtained from experimental tests. Weisgerber used this yield surface with the isotropic hardening rule to solve some plane strain problems of concrete. Alsanusi [5] analyzed some reinforced concrete problems using a second quasi-Tresca yield surface.

The second quasi-Tresca yield surface was generalized into three-dimensional stress state by Nazem [6]. The proposed yield surface is shown in Figure 2. The parameters in the second quasi-Tresca yield surface are used to define the yield surface. Note that the yield surface is defined in tension and compression regions separately according to the equations below:

Tension sides:

$$T_1 = a\beta_1\sigma_1 + a(1 - \beta_1)\sigma_2 - \beta_1\sigma_3 - a\beta_1\sigma(k) = 0,$$

$$T_2 = a(1 - \beta_1)\sigma_1 - \beta_1\sigma_2 + a\beta_1\sigma_3 - a\beta_1\sigma(k) = 0,$$

$$T_3 = a\beta_1\sigma_1 - \beta_1\sigma_2 + a(1 - \beta_1)\sigma_3 - a\beta_1\sigma(k) = 0,$$

$$T_4 = a(1 - \beta_1)\sigma_1 + a\beta_1\sigma_2 - \beta_1\sigma_3 - a\beta_1\sigma(k) = 0,$$

$$T_5 = -\beta_1\sigma_1 + a(1 - \beta_1)\sigma_2 + a\beta_1\sigma_3 - a\beta_1\sigma(k) = 0,$$

$$T_6 = -\beta_1\sigma_1 + a\beta_1\sigma_2 + a(1 - \beta_1)\sigma_3 - a\beta_1\sigma(k) = 0. \tag{8}$$

Compression sides:

$$C_1 = a\beta_2\sigma_1 - (1 - \beta_2)\sigma_2 - \beta_2\sigma_3 - a\beta_2\sigma(k) = 0,$$

$$C_2 = -(1 - \beta_2)\sigma_1 - \beta_2\sigma_2 + a\beta_2\sigma_3 - a\beta_2\sigma(k) = 0,$$

$$C_3 = -a\beta_2\sigma_1 - \beta_2\sigma_2 - (1 - \beta_2)\sigma_3 - a\beta_2\sigma(k) = 0,$$

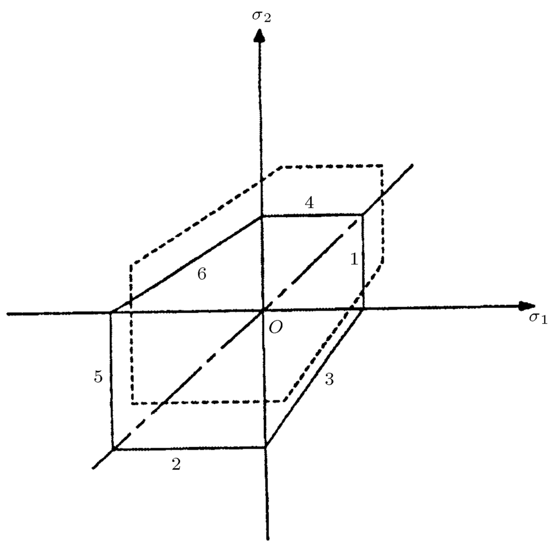

Figure 1. First quasi-Tresca yield surface.

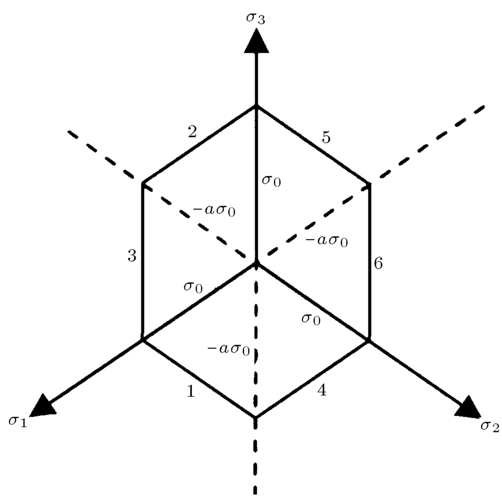

Figure 2. Proposed yield surface on π plane.

$$C_4 = -(1-\beta_2)\sigma_1 + a\beta_2\sigma_2 - \beta_2\sigma_3 - a\beta_2\sigma(k) = 0,$$

$$C_5 = -\beta_2\sigma_1 - (1-\beta_2)\sigma_2 + a\beta_2\sigma_3 - a\beta_2\sigma(k) = 0,$$

$$C_6 = -\beta_2\sigma_1 + a\beta_2\sigma_2 - (1-\beta_2)\sigma_3 - a\beta_2\sigma(k) = 0. \tag{9}$$

The above yield surface was used in the analysis of some three-dimensional problems by Rezaee-Pajand and Nazem [2]. The yield function is specifically suitable for materials showing different behavior under tension and compression as concrete.

ANALYSIS METHOD

In this study, the yield surface introduced by Rezaee-Pajand and Nazem [2] is used in solving reinforced concrete problems. The analysis benefits the incremental theory of plasticity in which a yield surface is initially defined and then a hardening rule is introduced. A flow rule is also required that determines the direction of plastic strains. An associative flow rule is used here, which assumes the yield function and plastic potential to be the same. The analysis performed is three-dimensional using eight-node brick elements representing the concrete and truss elements for reinforcement.

A program, based on object-oriented methodology using C++ language, was developed to analyze the nonlinear reinforced concrete problems. The time-stepping algorithm is based on the modified Newton-Raphson method in which the global system of equations is solved only once at each increment. The nonlinear finite element equation to be solved is [7]:

$$[\mathbf{K}^t]\{\mathbf{U}\} = \{\mathbf{R}^{t+\Delta t}\} - \{\mathbf{F}^t\}, \tag{10}$$

in which $\mathbf{K}$ is the stiffness matrix; $\mathbf{R}$ represents the vector of external nodal forces; $\mathbf{F}$ is the vector of internal nodal forces; $\mathbf{U}$ denotes the displacement vector; and t specifies the time.

Eight-Node Brick Element

Choosing an element type is a very important issue in the finite element method. The time spent for setting up the stiffness matrix can be reduced if the stiffness matrix of each individual element is calculated explicitly. Precision, on the other hand, is important to reduce the error of analysis. In the finite element study performed here, an eight-node brick element is used that has six perpendicular sides and which is shown in Figure 3. Selby [8] has shown that this type of element can provide good results in the analysis of concrete structures. Axes of Cartesian coordinates are parallel to element sides and, for simplicity, the origin is chosen at the centre of the element. This element includes eight nodes with three displacement degrees of freedom at each node.

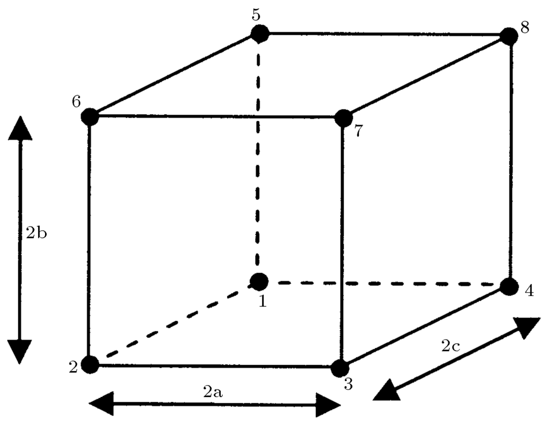

Figure 3. Eight-node brick element.

Modeling of the Reinforcement

To model the reinforcing bars, truss elements are used in this study which consist of two nodes with three translational degrees of freedom at each node. In this model, the compatibility of displacements between the bars and the concrete is satisfied at nodal points. Where required, the truss elements are added between nodal points on the concrete elements, being embedded with the finite element mesh to represent the reinforcing bars. This kind of modeling is widely used by researchers, as it provides a bond between the reinforcement and the concrete at nodes and does not permit any slip between the two materials [9]. The only shortcoming of the model, which usually occurs in complicated reinforced structures, is that the truss elements have to pass through concrete elements. However, for problems solved in this study, this drawback is not necessarily considered as an issue.

The stress-strain relation of steel is defined by the following equations:

$$f_s = E_s.\varepsilon_s, \qquad 0 \le \varepsilon_s \le \varepsilon_y,$$

$$f_s = f_y, \qquad \varepsilon_y \le \varepsilon_s \le \varepsilon_h,$$

$$f_s = f_y + \frac{f_u - f_y}{\varepsilon_u - \varepsilon_h}(\varepsilon_s - \varepsilon_h), \qquad \varepsilon_h \le \varepsilon_s \le \varepsilon_u, \tag{11}$$

in which f_s and ε_s are, respectively, the axial stress and the strain in steel bars; f_y and ε_s denote the yield stress and yield strain of steel; ε_h depicts the strain beyond which the strain-hardening of steel begins in a one-dimensional tension test; and f_u and ε_u represent, respectively, the ultimate stress and the ultimate strain that can be reached by a steel bar. The three equations in Equations 11 define three regions in a one-dimensional stress-strain space: an elastic region, a perfectly plastic region and a strain-hardening region, respectively. Such a trilinear function is very popular in the analysis of reinforced concrete structures by the finite element method [10].

Incremental Theory of Plasticity

According to the theory of plasticity, the constitutive equations governing the elastoplastic behavior of a material are usually derived based upon the following assumptions:

- The incremental strain tensor, $\dot{\varepsilon}$, can be decomposed into an elastic part, $\dot{\varepsilon}^e$, and a plastic part, $\dot{\varepsilon}^p$. Note that a superimposed dot represents the time derivative of a variable.

$$\dot{\varepsilon} = \dot{\varepsilon}^e + \dot{\varepsilon}^p. \tag{12}$$

- The elastic domain is described by a yield surface of the form $f(\boldsymbol{\sigma}, \boldsymbol{\kappa}) = 0$ where $\boldsymbol{\sigma}$ is the Cauchy stress tensor and $\boldsymbol{\kappa}$ represents a set of hardening parameters.
- Once plastic yielding occurs, the consistency condition requires that the stress state must remain on the yield surface as the plastic deformation occurs, such as:

$$\dot{f} = \frac{\partial f}{\partial \boldsymbol{\sigma}}.\dot{\boldsymbol{\sigma}} + \frac{\partial f}{\partial \boldsymbol{\kappa}}.\dot{\boldsymbol{\kappa}} = 0. \tag{13}$$

- The direction of plastic strains is normal to a surface called the plastic potential, g. This rule is known as the associated flow for $f = g$ and non-associated flow for $f \neq g$, and is expressed as:

$$\dot{\varepsilon}^p = \dot{\boldsymbol{\lambda}}.\frac{\partial g}{\partial \boldsymbol{\sigma}}, \tag{14}$$

where $\dot{\boldsymbol{\lambda}}$ is a positive scalar called the plastic multiplier.

- With the decomposition of the strains, the stress rate can be expressed by:

$$\dot{\boldsymbol{\sigma}} = \mathbf{C}^e.\dot{\varepsilon}^e, \tag{15}$$

where $\mathbf{C}^e$ represents the elastic stress-strain matrix.

- According to a mixed hardening rule which is a combination of isotropic hardening and kinematic hardening, the rate of transition of the yield surface in stress space, $\dot{\boldsymbol{\alpha}}$, is defined by:

$$\dot{\boldsymbol{\alpha}} = H(1-m)\dot{\varepsilon}^p, \tag{16}$$

where H is a constant and m represents the contribution of each of the isotropic and kinematic hardening rules into the mixed hardening rule. Note that, if $m = 1$, the hardening rule will be isotropic and for $m = 0$ a kinematic hardening rule will be obtained. The plastic strain rate can now be decomposed into an isotropic part, $\dot{\varepsilon}^{p(i)}$, and a kinematic part, $\dot{\varepsilon}^{p(k)}$, as:

$$\dot{\varepsilon}^p = \dot{\varepsilon}^{p(i)} + \dot{\varepsilon}^{p(k)},$$

$$\dot{\varepsilon}^{p(i)} = m\dot{\varepsilon}^p,$$

$$\dot{\varepsilon}^{p(k)} = (1-m)\dot{\varepsilon}^p. \tag{17}$$

The standard elastoplastic constitutive relation is obtained by:

$$\dot{\boldsymbol{\sigma}} = \mathbf{C}^{\mathrm{ep}}.\dot{\varepsilon}, \tag{18}$$

where $\mathbf{C}^{\mathrm{eq}}$ represents the elastoplastic stress-strain matrix. Given a strain increment, Equation 18 must be integrated during each time step to find out the stress increment.

NUMERICAL EXAMPLES

To show the ability of the finite element formulation suggested in this study, three numerical examples are presented in this section. These examples are: a reinforced concrete deep beam, a reinforced concrete slab and a reinforced concrete shear panel.

Reinforced Concrete Deep Beam

The first problem is a reinforced concrete deep beam. This problem was solved by Cervera [11]. This deep beam and its reinforcement are shown in Figure 4; the beam carries a uniform load on the top. The compressive and tensile strength of the concrete are assumed to be 14 MPa and 2.5 MPa, respectively. The yield stress of reinforcement is 320 MPa and the modulus of elasticity of bars is 2×10^5 MPa. The finite

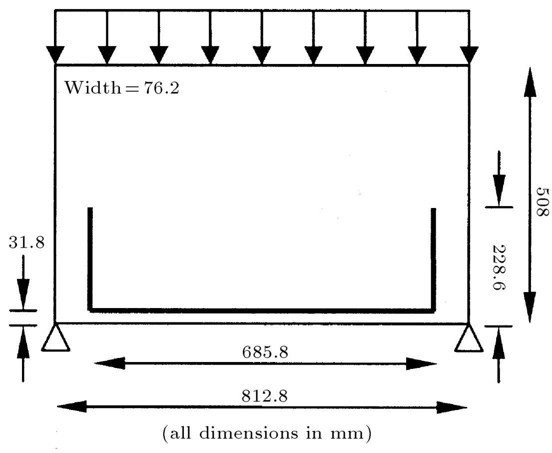

Figure 4. Reinforced concrete deep beam.

element mesh used in this analysis is shown in Figure 5. Only one half of the beam is considered in the analysis due to symmetry. Figure 6 illustrates the plot of the applied force versus the displacement of the midspan of the beam. Good agreement between previous analyses and the current analysis can be seen.

Reinforced Concrete Slab

The second example includes a reinforced concrete slab, which has been solved by Cervera [11]. The slab is composed of two reinforcement meshes at the top and the bottom. A concentrated load is applied at the centre of the slab, at point A, as depicted in Figure 7. The compressive and tensile strength of concrete is taken as 34 MPa and 2.5 MPa, respectively. The yield stress and Young's modulus of steel are assumed to be 670 MPa and 201000 MPa. One quarter of the slab is considered in analysis due to symmetry and the slab is divided into four layers, each including 25 elements. 120 truss elements are used for modeling the reinforcement at the top and bottom of the slab. The finite element mesh of the slab is shown in Figure 8. The plot of the applied concentrated load versus the displacement of a node under the applied load, obtained from nonlinear analysis, is shown in Figure 9. The results show the ability of the proposed model for the analysis of reinforced concrete structures.

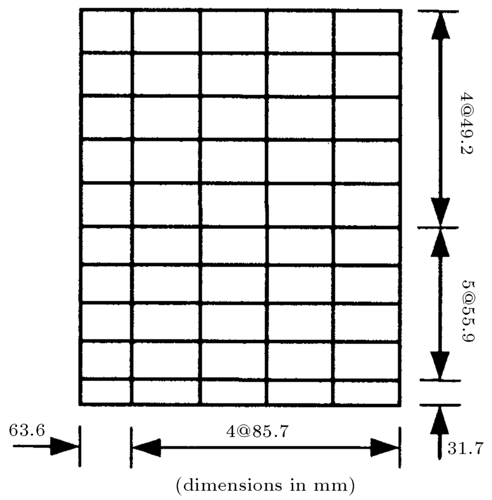

Figure 5. Finite element mesh of deep beam.

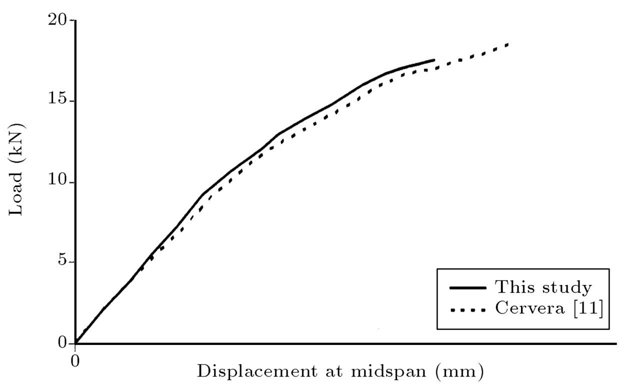

Figure 6. Load-displacement plot of deep beam.

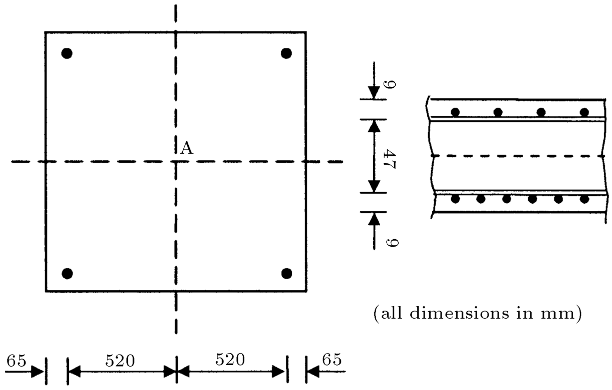

Figure 7. Reinforced concrete slab.

Shear Panel

Vecchio and Collins [12] studied the behavior of reinforced concrete shear panels. They tested 30 panels with different loadings and ratios of reinforcements. One of these panels is selected in this paper and is shown in Figure 10. The reinforcement consists of perpendicular bars with a ratio of 0.01785 and the panel is under shear stresses (Figure 10). The compressive and tensile strength of concrete are 20.5 MPa and 2.4 MPa, respectively. The Poisson ratio of concrete is taken as 0.15. The yield stress and Young's modulus of reinforcement are 442 MPa and 2×10^5 MPa, respectively. The finite element mesh for this example includes 25 brick elements and 80 truss elements as illustrated in Figure 11. The diagram of the shear stress versus the shear strain of the specimen is plotted

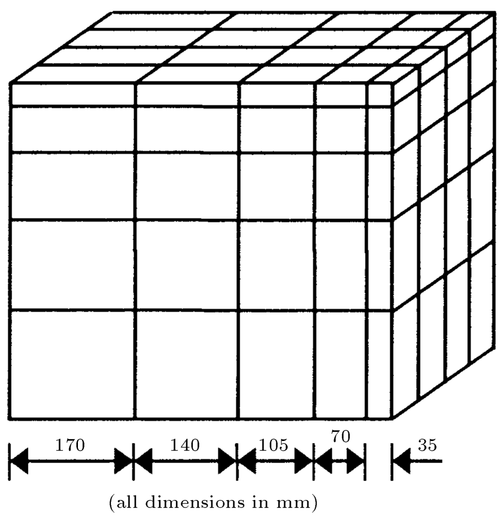

Figure 8. Finite element mesh of slab.

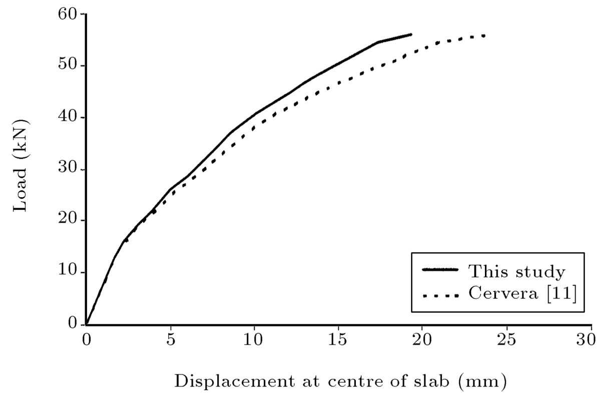

Figure 9. Applied load versus displacement of centre of slab.

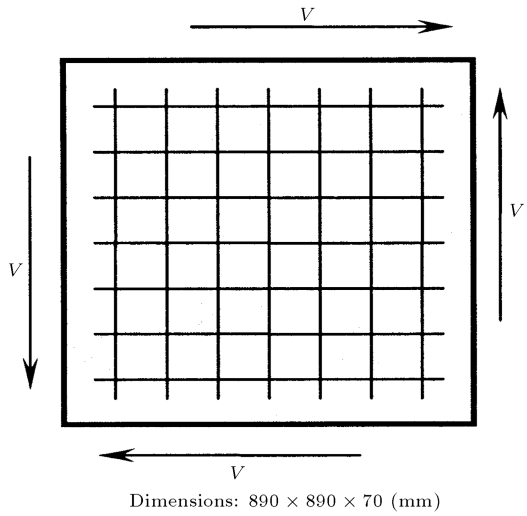

Figure 10. Shear panel specimen.

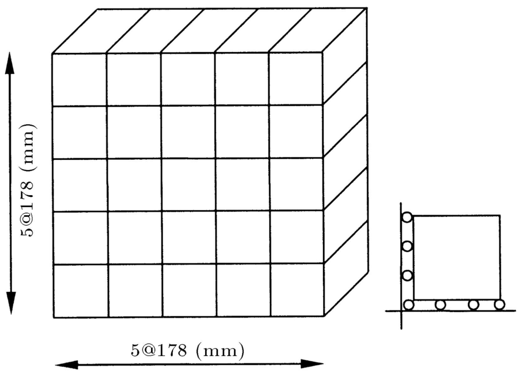

Figure 11. Finite element mesh of shear panel with boundary conditions.

in Figure 12. The results show reasonable agreement between the current analysis and experimental testing.

CONCLUSIONS

A nonlinear three-dimensional analysis of reinforced concrete structures was presented in this paper. A recently proposed yield surface, based on quasi-Tresca

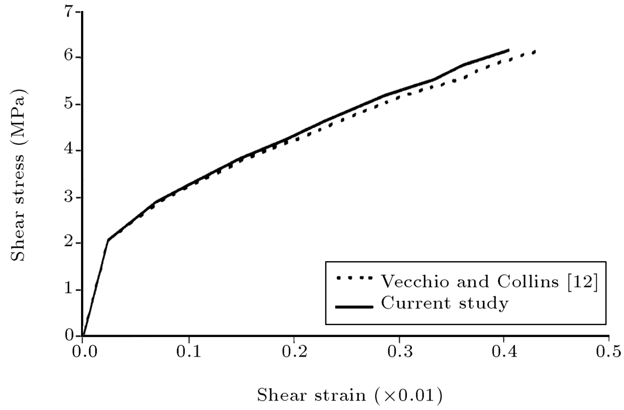

Figure 12. Shear stress versus shear strain of specimen.

models, was used in the analysis and considerable results were obtained. The reinforcements were modeled using simple truss elements. The current formulation is simple and can be implemented into a finite element code easily. Eight-node brick elements were used and their capability in the three-dimensional finite element analysis was demonstrated. Results indicate that the quasi-Tresca yield surface proposed by Rezaee-Pajand and Nazem [2] can be used in the nonlinear analysis of reinforced concrete structures.

REFERENCES

1. Chen, W.F., *Evaluation of Plasticity-Based Constitutive Models for Concrete Materials*, Oxford University Press, England (1988).
2. Rezaee-Pajand, M. and Nazem, M. "Elasto-plastic analysis of three-dimensional structures", *Engineering Computations*, **20**(3), pp. 274-295 (2003).
3. Rezaee-Pajand, M. "Uniaxial symmetrical Tresca yield condition in elasto-plastic finite element analysis", MSc Thesis, University of Pittsburgh (1979).
4. Weisgerber, F.E. "Elastic-plastic analysis for tension-weak materials using a linearized yield surface", *Research Report Performed While Occupying a Junior Morrow Research Chair*, Summer/Autumn Quarters (1981).
5. Alsanusi, S.K. "Elasto-plastic analysis of plane stress problems using linearized yield surface and mixed hardening", PhD Dissertation, University of Pittsburgh (1987).
6. Nazem, M. "Nonlinear analysis of three dimensional continuous structures", MSc Thesis, Ferdowsi University of Mashad, Iran (1997).
7. Bathe, K.J., *Finite Element Procedures*, Prentice Hall, New Jersey (1996).
8. Selby, R.G. "Nonlinear finite element analysis of reinforced concrete solids", MSc Thesis, University of Toronto (1990).
9. Cheng, Y.M. and Fan, Y. "Modeling of reinforcement in concrete and reinforcement confinement coefficient",

Finite Elements in Analysis and Design, **13**, pp. 271-284 (1993).

10. Polak, M.A. and Vecchio, F.J. "Nonlinear analysis of reinforced concrete shells", *Journal of Structural Engineering*, **119**(12), pp. 3439-3462 (1993).
11. Cervera, M., Hinton, E. and Hassan, O. "Nonlinear analysis of reinforced concrete plates and shell structures using 20-noded isoparametric brick elements", *Computers and Structures*, **25**(6), pp. 845-869 (1987).
12. Vecchio, F.J. and Collins, M.P., *The Response of Reinforced Concrete to Inplane Shear and Normal Stresses*, University of Toronto, Department of Civil Engineering, Publication No. 82-03 (1982).